Neutron Diffraction by Liquid Zinc*

B. A. Dasannacharya,† Q. O. Navarro, H. Ibarra, S. Chatraphorn,‡ and G. B. Lee§
Philippine Atomic Research Center, Diliman, Quezon City, Philippines
(Received 11 October 1968; revised manuscript received 8 January 1968)

The paper presents results on neutron diffraction by liquid zinc at 450°C. The measured structure factor differs greatly from the x-ray structure factor reported earlier, but agrees reasonably well with a theoretical Percus-Yevick structure factor for hard spheres. The electrical resistivity calculated using our structure factor is about half of the measured value. It does not seem that this large difference can be accounted for by small errors in the structure factor or the pseudopotential. Inadequacy of the Born approximation has been suggested as one possible cause of this disagreement, the other being rather large errors in the calculated pseudopotentials. The possibility of the existence of a law of corresponding states between various liquids is examined and found to be unlikely. An effort to explain the structure with a quasicrystalline model has met with qualitative success.

INTRODUCTION

Diffraction of x rays by liquids has been a subject of considerable interest for several decades,[1,2] mainly from the point of view of getting an insight into their static structures. Neutron diffraction, on the other hand, though comparatively new, has given useful information especially for some liquids which are not very amenable to x-ray scattering experiments. The interest in these experiments has grown considerably, after it was shown that the structure factor involved is connected in a direct way with the dc electrical resistivity of the liquid metal. In this paper we present results of our measurements on diffraction of neutrons from liquid zinc at 450°C. Only one x-ray diffraction measurement on liquid zinc has been reported earlier.[3,4] This measurement showed an unusual structure factor in the sense that a hump was found before the main diffraction peak. This has not been observed in any other metal.

In Sec. I we present briefly the experimental setup and the observations. The derived pair correlation function is presented in Sec. II. In Sec. III, the structure factor is described in terms of the Percus-Yevick formulation for hard spheres and the dc electrical resistivity is derived from the measured structure factor and a pseudopotential due to Animalu and Heine. In addition, the possibility of using a law of corresponding states is discussed, and finally, the data is fitted using a quasicrystalline model. Section IV gives a summary.

I. APPARATUS AND EXPERIMENTAL DETAILS

The measurements were carried out at the 1-MW swimming pool reactor PRR-1, at the Philippines Atomic Research Center, using a conventional neutron diffractometer[5] which gives incident neutrons of 1.17 Å.

Zinc of 99.8% purity was sealed in vacuum in a Vycor tube of 10-mm inner diameter and 1.5-mm wall thickness. The sample was heated by means of two heaters, one at the top of the Vycor tube and another at the bottom. The temperature was read using thermocouples attached to each of these two heaters. The whole assembly was held in a vacuum chamber after having been covered by a thin aluminum radiation shield. The sample was kept at 450°C.

Figure 1(a) shows the diffraction pattern. The dots show the raw pattern and the crosses show the corresponding background with the empty Vycor casette. The net pattern is shown in Fig. 1(b) after applying corrections for the empty

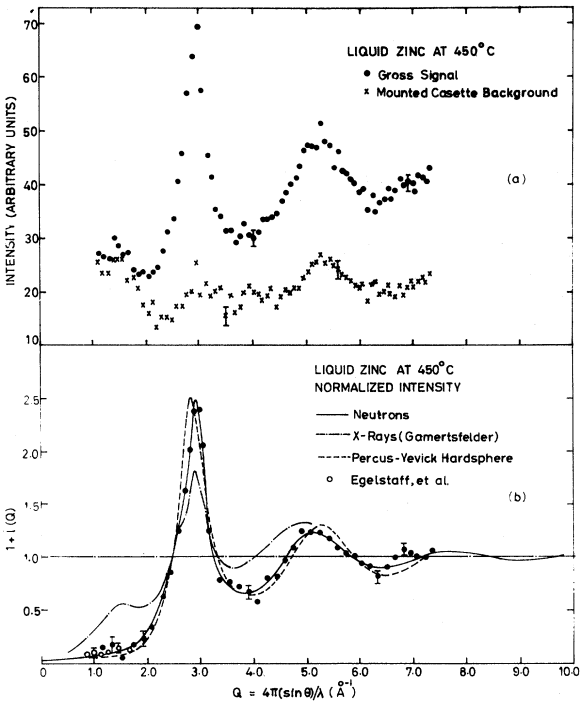

FIG. 1. (a) The signal (zinc + container) (o) and empty container (x) counts in arbitrary units when 1.17 Å neutrons are scattered from them. (b) The normalized net counts (o) with the bars showing the statistical errors; open circles show earlier neutron results of Egelstaff *et al.* (Ref. 17) with bars showing the systematic plus statistical errors; the thick line is the final extended structure factor used for calculating the pair correlation function; the dashed line is the result of a Percus-Yevick hard-sphere model calculation, and the long- and short-dashed line is the x-ray structure factor (Ref. 3).

casette[6] and multiple scattering.[7] In our case we find that the multiple scattering is about 15% of the primary scattering. The casette contribution, on the other hand, should be less than that shown in Fig. (1) because of the transmission of the neutrons through the sample. This reduction is about 20% of the measured empty casette intensity and, after taking account of fast-neutron background, is almost entirely compensated by the presence of multiple scattering. We have, therefore, subtracted the empty casette counts without any correction. The pattern is a total of several runs, and the errors shown are only due to statistics. The measurements are carried out up to a wave-vector transfer of about 7.3 Å^{-1} which is the maximum wave-vector transfer attainable with the present setup.

II. RESULTS

A. Structure Factor and Pair Correlation Function

The intensity of neutrons of wavelength λ getting scattered through an angle 2θ is given by the well-known expression

$$I(Q)=I_{\text{inc}}+I_{\text{coh}}(Q)=N[\langle b^2\rangle-\langle b\rangle^2]+N\langle b\rangle^2\{1+[(N-1)/V]\times 4\pi\int_0^\infty[g(r)-1]r^2\frac{\sin Qr}{Qr}dr\}, \quad (1)$$

where I_{inc} and $I_{\text{coh}}(Q)$ denote the isotropic incoherent and the angle-dependent coherent scattering at the wave-vector transfer $Q=4\pi(\sin\theta)/\lambda$, N gives the number of particles in a volume V, $\langle b\rangle$ represents the average scattering amplitude of the scattering centers, and $g(r)$ gives the pair correlation function. We can rewrite Eq. (1) as

$$I(Q)=I_{\text{inc}}+[I(\infty)-I_{\text{inc}}]\{1+[(N-1)/V]\times 4\pi\int_0^\infty[g(r)-1]r^2[(\sin Qr)/Qr)]dr\}, \quad (2)$$

where $I(\infty)\equiv\langle b^2\rangle$ gives the total scattering at large Q. This leads to the structure factor $i(Q)+1$, given by

$$i(Q)=\frac{I(Q)-I(\infty)}{I(\infty)-I_{\text{inc}}}=4\pi n\int[g(r)-1]r^2\frac{\sin Qr}{Qr}dr. \quad (3)$$

Fourier-transforming this, one obtains

$$n[g(r)-1]=(1/2\pi^2)\int Q^2 i(Q)[(\sin Qr)/Qr)]dQ, \quad (4)$$

where n is the atomic number density. One notices from Eq. (3) that an absolute measurement is not necessary since $i(Q)$ is a ratio. This may, however, be desirable in certain cases.[8] Further, to get the structure factor one should know two constants—I_{inc} and $I(\infty)$.

The most common method for getting I_{inc} in neutron measurements is to smoothly extrapolate the measured pattern at small Q to the forward direction and correct for $I_{\text{coh}}(0)$, which can be easily estimated from the known isothermal compressibility. Once this is known, one uses the fact that the correlation function $g(r)$ is zero at $r=0$ to get the second constant $I(\infty)$. This gives, from Eq. (4),

$$-2\pi^2 n=\int\{[I(Q)-I(\infty)]/[I(\infty)-I_{\text{inc}}]\}Q^2dQ \quad (5)$$

$$\text{or}\quad I(\infty)=\frac{\int_0^{Q_{\max}}Q^2I(Q)dQ}{\frac{1}{3}Q_{\max}^2-2\pi^2n}-\frac{2\pi^2nI_{\text{inc}}}{\frac{1}{3}Q_{\max}^2-2\pi^2n}, \quad (6)$$

where $Q_{\max}$ is the maximum value of the wave-vector transfer up to which measurements have been carried out. Since zinc scatters coherently, our problem simplifies to the extent that the second term in Eq. (6) drops out.

As a starting point, we got an $I(\infty)$ from Eq. (6) less the second term, and used this to normalize the data and get the structure factor. The smooth $i(Q)$ was then used to obtain the first $g(r)$ on an IBM-1620 computer by feeding in the structure factor at $\Delta Q=0.1$ Å^{-1}, and using Simpson's rule for performing the integration. Since our measurements are confined only up to about 7.3 Å^{-1}, we felt it advisable to use the methods suggested by Kaplow *et al.*[9] to increase the range of Q for $i(Q)$. Accordingly, we extended the data up to $Q=15.0$ Å^{-1} by performing integrations back and forth between $i(Q)$ and $g(r)$. The final $i(Q)$ and $g(r)$ are shown with solid lines in Figs. 1(b) and 2 respectively. The $i(Q)+1$ up to roughly $2k_F$, where k_F is the Fermi wave vector is listed in Table I, and some relevant numbers related to $g(r)$ are listed in Table II.

B. Errors

The errors involved in the measurements and the analysis of this kind have been discussed extensively in literature (see Ref. 2 for details) in connection with both x-ray and neutron scattering.[8] We would like to make only a couple of general remarks which seem relevant but have not been sufficiently emphasized. The first point is with regard to the determination of I_{inc}. It has been noted[2,10] that a small error in I_{inc}, due to an error in extrapolation at small Q, will introduce only a very small error in $g(r)$ because the integrand in Eq. (4) involves a product of Q and $i(Q)$. This, while reasonable for x rays, seems misleading for the neutron case for the following reason. It can be easily seen, by considering the relative magnitudes of the various terms in Eq. (5), that a small change ΔI in I_{inc} will not change $I(\infty)$ appreciably. The net result of this, therefore, will be to change the $i(Q)$ in Eq. (4) from $[I(Q)-I(\infty)]/[I(\infty)-I_{\text{inc}}]$ to $[I(Q)-I(\infty)]/I(\infty)-I_{\text{inc}}-\Delta I]$. If, for example, ΔI is 5% of $I(\infty)-I_{\text{inc}}$, which is not uncommon in measurements, $i(Q)$ will change by 5% *throughout* the range of measurements [and so also will $g(r)$]. This effect, therefore, will not be confined to small Q even though the extrapolation is made in that region.

The second point concerns with the determination of the two normalization constants using a crite-

TABLE I. Structure factor of liquid zinc at 450° C.

Q (Å^{-1})	$i(Q)+1$	Q (Å^{-1})	$i(Q)+1$	Q (Å^{-1})	$i(Q)+1$
0.0	0.016	1.1	0.065	2.2	0.518
0.1	0.020	1.2	0.076	2.3	0.680
0.2	0.024	1.3	0.084	2.4	0.848
0.3	0.028	1.4	0.092	2.5	1.063
0.4	0.031	1.5	0.108	2.6	1.306
0.5	0.035	1.6	0.127	2.7	1.684
0.6	0.039	1.7	0.146	2.8	2.202
0.7	0.043	1.8	0.173	2.9	2.429
0.8	0.046	1.9	0.216	3.0	2.202
0.9	0.050	2.0	0.291	3.1	1.565
1.0	0.054	2.1	0.389	3.2	1.090

TABLE II. Positions and magnitudes of peaks and valleys in $H(r)=4\pi r^2 n\,[g(r)-1]$. r is in Å and $H(r)$ in atoms/Å. I gives the number of atoms under the first peak of $4\pi r^2 n g(r)$.

r	$H(r)$	r	$H(r)$	r	$H(r)$	$I=n\int_{r_1}^{r_2}4\pi r^2 g(r)\,dr$
2.71	7.3	7.00	3.5	11.30	2.4	$r_1=2.00$
3.62	4.2	8.04	3.2	12.35	2.15	$r_2=3.53$
4.90	3.8	9.10	3.0	13.44	1.7	$I=10.98$
5.90	3.95	10.26	2.65	14.64	1.7	

rion suggested by Rahman[11] and used by different authors in some recent papers.[12,13] Dasannacharya and Rao[14] have examined this in some detail and conclude that it is enough to consider the case when $\mu=0$, in that test. With this specialization the criterion reduces to

$$-n\int_0^L 4\pi r^2[g(r)-1]dr = (2/\pi)\int_0^\infty Qi(Q)\int_0^L r\sin Qr\,dQ\,dr \qquad (7a)$$

$$\text{or}\quad -n=\frac{1}{2\pi^2}\int_0^\infty Q^2 i(Q)\frac{3(\sin QL-QL\cos QL)}{(QL)^3}dQ \quad \text{for } L<r_c\,, \qquad (7b)$$

where r_c is the so-called distance of closest approach, below which $g(r)$ is zero. Physically, this condition is derived from the fact that the total number of atoms, excluding the one at the origin, is zero below $r=r_c$. A much simpler criterion comes out, however, when one uses the fact that $g(r)$ itself is zero [instead of $\int 4\pi r^2 g(r)dr=0$]. This gives

$$-n=\frac{1}{2\pi^2}\int_0^\infty Q^2 i(Q)\frac{\sin QL}{QL}dQ \text{ for } L<r_c\,. \qquad (8)$$

One will immediately notice that this is Eq. (4) itself, in the region of $r<r_c$. With reference to the correlation function, it means that there are no ripples in $g(r)$ [or $4\pi r^2 g(r)$] in the region of $r<r_c$. If this condition holds, Eq. (7) will automatically be satisfied.[15] Hence, it is enough to try to get a $g(r)$ which is free from ripples at small r. This has been also the criterion followed by Kaplow *et al.*

In our case we started with an $I(\infty)$ given by Eq. (4) with the experimental value for n and tried to reduce the ripples by extending the data and modifying the normalizing constant up to an arbitrary point. The final $g(r)$ is presented in Fig. 2. Figure 3 shows the effect on the $g(r)$ of

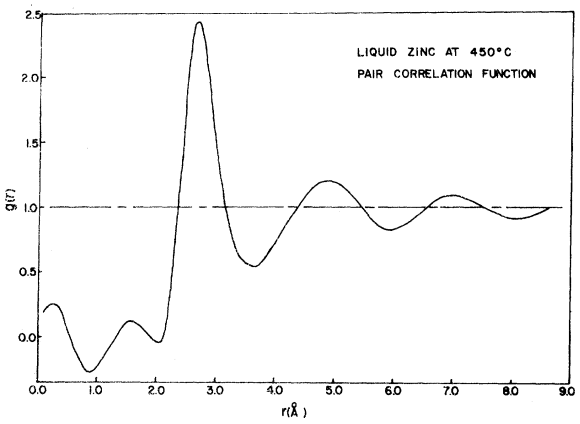

FIG. 2. The pair correlation function for liquid zinc at 450°C.

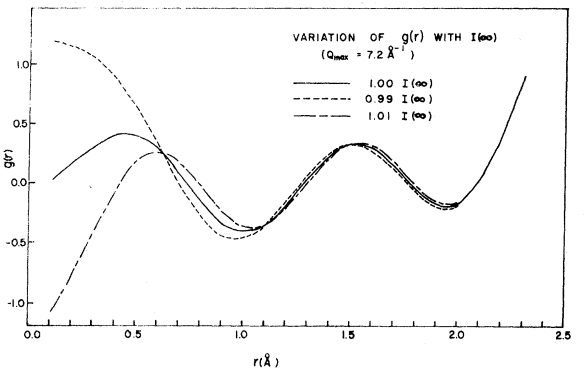

FIG. 3. The effect of a 1% change in $I(\infty)$ on the pair correlation function.

changing $I(\infty)$ by 1%, and clearly brings out the sensitivity of the ripples to this quantity. Incidentally, this also shows why we plot $g(r)$ and not $rg(r)$ or $4\pi r^2 g(r)$. The plots of $rg(r)$ or $4\pi r^2 g(r)$ tend to suppress the oscillations at small r and do not clearly bring out the extent of the errors (compare Figs. 2 and 5). The value of n calculated by taking the best line through the points below $r = r_c$ comes out to be 0.057×10^{24} atoms/cc. This is roughly 5% lower than the measured density.[16]

III. DISCUSSION

We will first make a few remarks about the structure factor itself. This has been measured earlier by x-ray diffraction,[3] and has been used by various authors to calculate the electrical resistivity of liquid zinc with good results. We have compared our measurements with x-ray structure factor in Fig. 1(b). The agreement is poor. The reason for this is not known. In the same figure, we have also plotted with open circles the results of some recent neutron measurements of Egelstaff *et al.*[17] The measurements were done specially to look at small wave-vector transfers. The errors on these points are statistical plus systematic. We notice a good agreement (also see Ref. 4).

We have also compared our results with a calculation in which a hard-sphere model is assumed for the liquid and the $i(Q)$ is evaluated using the Percus-Yevick formulas [Fig. 1(b), dashed lines]. The explicit formulas have been given by Ashcroft and Lekner,[18] and we have calculated the curve for the case when the packing density for hard spheres is assumed to be 45%. This packing density for hard spheres, according to Ashcroft and Lekner, gives the best fit to the structure-factor data for most of the liquids. It is also possible to calculate the packing density from the experimental density and the position of the first peak in the radial distribution function.[13] This comes to 45.5% for zinc. Our data can be fitted fairly well with a hard-sphere diameter of 2.43 Å as calculated from the measured density, 0.0597 atoms/Å^3, of the liquid.

Coming now to the question of calculating the resistivity of liquid zinc, Ziman[19] and Bradley *et al.*[20] have shown that to the lowest order in perturbation, the resistivity ρ of liquid metals is given by the relation

$$\rho = \frac{3\pi m^2}{e^2 n \hbar^3 k_F^2}\left(\frac{1}{4k_F^4}\int_0^{2k_F} V^2(Q)[i(Q)+1]Q^3 dQ\right), \quad (9)$$

where $V(Q)$, $i(Q)+1$, and k_F are the Fourier transform of the screened pseudopotential, the structure factor, and the Fermi wave vector, respectively, for the liquid. Using the Fourier transform of the pseudopotential as given by Animalu and Heine,[21] but modified for the change in density, we have calculated the resistivity of liquid zinc at 450°C. The calculated value comes out to be 19.1 $\mu\Omega$ cm as compared with an experimental value of 37.4 $\mu\Omega$ cm. The resistivity was also calculated for the case when $V(Q)$ was changed by 0.01 Ry throughout. On subtracting 0.01 Ry the resistivity changes to 18.4 $\mu\Omega$ cm, and, on adding, the value increases to 22.0 $\mu\Omega$ cm. Therefore, the maximum difference due to these changes is 13%.

The resistivity of liquid zinc has been calculated several times earlier,[18,22–26] and these are summarized in Table III along with the potential and the structure factors used in these calculations. It is not surprising that our calculated value is similar to that given by Ashcroft and Lekner, since our structure factor is reasonably well described by a Percus-Yevick formula for hard spheres. It is also noticeable in the same table that all the calculations using the x-ray diffraction pattern give a reasonable agreement with the experimental value. Whatever the potential used, the calculated value is within ± 20% of an average calculated value of 39 $\mu\Omega$ cm. In fact it was shown first by Springer,[24] and then by Wiser,[26] that the variation in the potential has maximum effect on the resistivity in the case of monovalent metals, and that it is much less for polyvalent metals. It seems reasonable to assume that it is not more than 25 to 30%. Our calculations confirm this as do those of Adams and Leach.[27] It therefore seems

TABLE III. Resistivity of liquid zinc calculated using several potentials and structure factors.

Reference (year)	Potential	Structure factor	Resistivity
22 (1963)	Ref. 22	x ray	39
24 (1964)	Fit to Ref. 22	x ray	35.3
24 (1964)	Fit to Ref. 22 {+0.01 Ry, −0.01 Ry}	x ray	{38.7, 34.0}
23 (1965)	Heine-Abarenkov[a]	x ray	44
25 (1965)	Ref. 21	x ray	41.6
26 (1966)	Ref. 22	x ray	36
26 (1966)	Ref. 22 {+0.015 Ry, −0.015 Ry}	x ray	{38, 37}
18 (1966)	Heine-Abarenkov[a]	Percus-Yevick hard sphere	16.6
18 (1966)	Ref. 21	Percus-Yevick hard sphere	18.6
Present work	Ref. 21	neutron	19.1
Present work	Ref. 21 {+0.01 Ry, −0.01 Ry}	neutron	{22.0, 18.4}

[a]V. Heine and I. Abarenkov, Phil. Mag. 9, 451 (1964).

certain that no minor change in the potential will bring about an agreement between the theory and the experiment.

It has also been pointed out[28] that any error in establishing the peak position correctly in the diffraction pattern will affect the resistivity to a very large extent. In our case, a uniform contraction of the diffraction pattern by an amount such that the first peak of $i(Q)$ changes by 0.1 Å^{-1} (~ 3.5%), increases the resistivity from 19.1 to 22.2 $\mu\Omega$ cm, that is, by about 16.5%. A change of 0.1 Å^{-1} in Q, however, corresponds to a fairly large and unlikely change of 1° in the scattering angle. This combined with an increase of 0.01 Ry in the potential brings the resistivity to 25.6 $\mu\Omega$ cm, which is still only about 70% of the experimental value.

In view of the above discussion, we are led to conclude that the good agreement obtained earlier between the experiment and the theory was fortuitous, and no small change in the pseudopotential will lead to the correct value for the resistivity. The answer to the discrepancy should be found either in a rather large change in potential or in a modification of the theoretical formulation itself. The latter course has been suggested by Greenfield[29] on the basis of his measurements of the temperature dependence of the x-ray structure factor in sodium, but several objections have been raised in that connection.

Finally, coming to the problem of the structure of the liquid, one can either try to describe the radial distribution function on the basis of a corresponding-states relation, or on that of a model. Paskin,[30] for example, argues for the cause of the corresponding states, and concludes that for many purposes the corresponding-states relation is probably good enough. The same idea is implied when Ashcroft and Lekner[18] use the Percus-Yevick theory for hard spheres, with a constant packing density, for calculating the resistivity of 25 metallic liquids. In our case we have done two types of comparison. First, we have compared our $4\pi r^2 n[g(r)-1]$ with the experimentally determined radial distribution functions for Pb, Hg, Sn, and Al. Second, we have calculated the radial distribution function based on the quasicrystalline model of Kaplow *et al.*[9]

Paskin has compared the radial distribution functions for Ar (fcc), Na, Rb, Cs (bcc), and In (tetragonal) using a scaling factor proportional to the cube root of the atomic volume, $(1/n)^{1/3}$. Fessler *et al.*[31] have compared Al, Pb (fcc), and Hg (rhombohedral). As the scaling factor, they have used the nearest neighbor distance obtained from a fit with the quasicrystalline model.[9] This will, however, not satisfy the necessary condition that the values of $4\pi r^2 n$ below the distance of closest approach should exactly correspond to each other for various elements obeying the law of corresponding states. We therefore follow Paskin in using a scaling factor $(1/n)^{1/3}$. It is worth mentioning here that if one wants to compare the radial distribution functions up to large distances it is important to select the proper scaling factor, since any small difference in this will get multi-

plied as one goes to larger r.

In our comparison, we will confine ourselves to the distances involved and will, for the moment, not consider the actual magnitudes of the radial distribution function. In Table IV we list the ratio r_A/r_B of the distances at which the respective peaks and valleys occur in elements A and B. We have also listed the ratio $(n_B/n_A)^{1/3}$ of the scaling factors, in the fifth row. If the corresponding-states relation holds, the numbers up to the fifth row in any column should be the same. This is obviously not the case. The difference in these numbers is as much as 15% when the comparison is made with Hg or Sn and 7% when the comparison is made with Pb or Al. It can be easily verified that these numbers will be constant (within 2%) only when one compares Al with Pb or Hg with Sn. Hence, we conclude that the law of corresponding states is not applicable in the form described above.

There are, however, some noteworthy features in the table. One can see that the first peak can always be described reasonably well by the scaling factor obtained from the density (row VII). Also, the ratio r_A/r_B, beyond the second peak, remains constant for any pair A/B. This can be seen from the fourth row in which we have given average ratio taken over a total of nine peaks and valleys. The maximum deviation is less than 2%. These conclusions are strikingly brought out by plotting these numbers as shown in Fig. 4. Here we plot individually, for different pairs of these five elements, the ratios of the positions of the peaks and valleys, instead of the average r_A/r_B. The shaded region gives the average of the last nine points (five valleys and four peaks) with a width of 2% on each side. Clearly the atomic scaling factor (the square) is beyond this region in all the cases except Pb/Al and Hg/Sn.

As mentioned earlier, our comparison applies only to the distances involved and not to the actual magnitudes of the radial distribution functions. This does not seem necessary since, within the present accuracy, the correspondence of magnitudes does not seem to hold even for substances like Pb and Al which have the same structure in the solid state.[31]

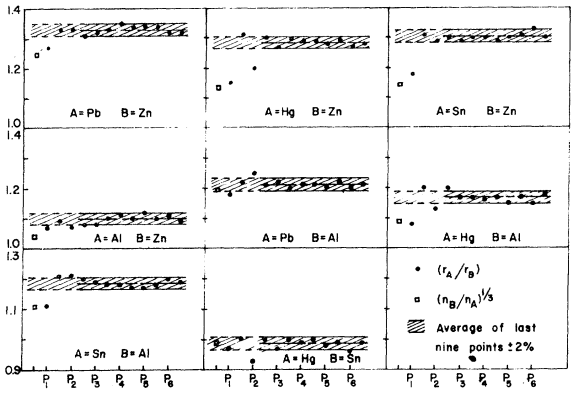

FIG. 4. Dots (o) show the ratio of the corresponding peak and valley positions in the radial distribution functions of elements A and B. The hatched region is the average of the last nine points, that is, the second valley to the sixth valley in the radial distribution function, with a 2% width on each side. The open square shows the cube root of the ratio of the densities and represents the atomic scaling factor. P_i is the ith peak index.

In view of the fact that a law of corresponding states cannot be found, we have tried to fit a specific model to our radial distribution function. We have chosen the quasicrystalline model because of its simple physical meaning. The procedure followed for the fitting was similar to that prescribed by Kaplow *et al.*[9] The solid lattice was first expanded uniformly in its linear dimension by 2% and then each δ function in the radial distribution function of the solid was broadened into a Gaussian and damped. Finally, the density was adjusted to the experimental value. The result is shown in Fig. 5 with dashed line. The full line shows the experimental $4\pi r^2 n[g(r)-1]$. The fit was done manually, and the final value shown

TABLE IV. Comparison of the radial distribution functions of different metals.

	r_A/r_B	*Pb/Zn*	*Hg/Zn*	*Sn/Zn*	*Al/Zn*
I	Peak 1	1.27	1.15	1.18	1.07
II	Valley 1	1.33	1.31	1.31	1.09
III	Peak 2	1.33	1.20	1.29	1.07
IV[a]		1.33 ± 0.020	1.28 ± 0.015	1.303 ± 0.02	1.099 ± 0.02
V	$(n_B/n_A)^{1/3}$	1.245	1.136	1.147	1.041
VI	[(IV−V)/V] × 100	+6.8	+11.0	+13.6	+5.6
VII	[(I−V)/V] × 100	+2.0	+1.2	+2.9	+2.2

[a]The ratio presented in this row is the average of the nine ratios from the second valley through to the sixth valley including the peaks in between.

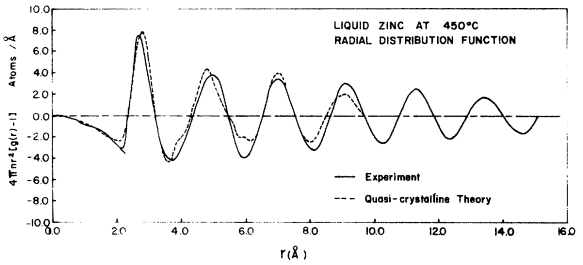

FIG. 5. Comparison of the experimental radial distribution function of zinc at 450°C with a calculation based on the quasicrystalline model.

is not necessarily the best possible. The figure clearly shows that the radial distribution function can be fitted reasonably by starting from the parent solid. The agreement is only qualitative and definite disagreement can be seen. The period of oscillations, however, is reproduced fairly well. Similar conclusions were reached by Kaplow *et al.*[9] and Fessler *et al.*[31]

In making the fit to our data we took the ratio $c/a = 1.856$, which is the value at room temperature. It is known that as the temperature increases, the ratio decreases towards the ideal value. However, zinc melts before the ideal value is reached. It would be of interest to see whether an ideal c/a ratio would give a fit to the data. We have not been able to do this because of the lengthy nature of these calculations.

IV. SUMMARY AND CONCLUSIONS

The structure factor $i(Q)+1$ for liquid zinc at 450°C has been measured using neutrons. The pair correlation function $g(r)$ and the radial distribution function $4\pi r^2 n[g(r)-1]$ have been derived from the structure factor. Both $i(Q)$ and $g(r)$ are very different from the x-ray measurements reported earlier, but are in good agreement with the neutron measurements. Our structure factor shows a reasonable agreement with the Percus-Yevick structure factor for hard spheres with a packing density of 45%.

The electrical resistivity derived from our data, using a pseudopotential due to Animalu and Heine, is roughly half of the experimental value. It does not seem possible to account for this large difference if reasonable allowances are made in the structure factor or the potential. The explanation may lie either in a large change in potential or in the breakdown of the Born approximation, as suggested earlier by Springer and Greenfield.

The radial distribution function for zinc is not related to Pb, Al, Hg, or Sn by a law of corresponding states of the type suggested by Paskin. However, after the first two peaks the positions of the peaks and valleys in the radial distribution functions of any two elements can be made to coincide within 2% by a single scaling factor. This factor is not related to the atomic volume in a simple manner. The radial distribution function for zinc can be described reasonably well by a quasicrystalline model up to 10 Å, though the agreement between the experiment and the model is not quantitatively adequate.

ACKNOWLEDGMENTS

We wish to acknowledge with thanks the help and cooperation rendered to this project by the Experimental Services Department and the Reactor Operations Department of the Philippines Atomic Research Center. We would also like to thank the Computer Center of the Mapua Institute of Technology for allowing us the use of their computer. The program for the computer was written by Mrs. V. P. Garchitorena.

---

*Work performed under the India-Philippines-IAEA joint project.

†Bhabha Atomic Research Center, Trombay, India.

‡The Office of the Atomic Energy for Peace, Bangkok, Thailand.

§Office of the Atomic Energy, Seoul, Korea.

[1]N. S. Gingrich, Rev. Mod. Phys. 15, 90 (1943).

[2]K. Furukawa, Rept. Progr. Phys. 25, 395 (1962).

[3]Gamertsfelder, J. Chem. Phys. 9, 450 (1941).

[4]G. Caglioti, M. Corchia, and G. Rizzi, Nuovo Cimento 49B, 222 (1967). This paper reports neutron diffraction measurements from liquid zinc and came to our attention after our paper was completed. The structure factor which is reported agrees very well with ours.

[5]Q. O. Navarro, M. G. Natera, and V. M. Pineda, Philippine Atomic Energy Commission Report No. PAEC (D) PH671, 1967 (unpublished).

[6]B. N. Brockhouse, L. M. Corliss, and J. M. Hastings, Phys. Rev. 98, 1721 (1955).

[7]I. A. Blech, and B. L. Averbach, Phys. Rev. 137, A1113 (1965).

[8]P. A. Egelstaff, in *The Proceedings of the International Conference on the Properties of Liquid Metals, Brookhaven National Laboratory* 1966, edited by P. D. Adams *et al.* (Taylor and Francis, Ltd., London, 1967).

[9]R. Kaplow, S. L. Strong, and B. L. Averbach, Phys. Rev. 138, A1336 (1965).

[10]P. Ascarelli, Phys. Rev. 143, 36 (1966).

[11]A. Rahman, J. Chem. Phys. 42, 3540 (1965).

[12]P. D. Randolph and K. S. Singwi, Phys. Rev. 152, 99 (1966).

[13]H. Ocken and C. N. J. Wagner, Phys. Rev. 149, 120 (1966).

[14]B. A. Dasannacharya and K. R. Rao, unpublished.

[15]It is possible to deduce a number of such criteria, which are necessary but not sufficient. All these criteria reduce to Eq. (5) for $L=0$. Equation (5) therefore seems the best starting point for normalization.

[16]*Handbook of Chemistry and Physics* (Chemical Rubber Publishing Co., Cleveland, Ohio, 1957).

[17]P. A. Egelstaff, C. Duffill, V. Rainey, J. E. Enderby, and D. M. North, Phys. Letters 21, 286 (1966).

[18]N. W. Ashcroft and J. Lekner, Phys. Rev. 145, 83 (1966).

[19]J. M. Ziman, Phil. Mag. 6, 1013 (1961).

[20]C. C. Bradley, T. E. Faber, J. M. Ziman, and E. G. Wilson, Phil. Mag. 7, 865 (1962).

[21]A. O. E. Animalu and V. Heine, Phil. Mag. 12, 1249 (1965); and A. O. E. Animalu, Cavendish Laboratory Technical Report No. 3, 1965 (unpublished).
[22]W. Harrison, Phys. Rev. 129, 2512 (1963).
[23]L. J. Sundstrom, Phil. Mag. 11, 657 (1965).
[24]B. Springer, Phys. Rev. 136, A115 (1964).
[25]A. O. E. Animalu, Phil. Mag. 11, 379 (1965).
[26]N. Wiser, Phys. Rev. 143, 393 (1966).
[27]P. D. Adams and J. S. Ll. Leach, Phys. Rev. 156, 178 (1967).
[28]N. C. Halder and C. N. J. Wagner, J. Chem. Phys. 45, 482 (1966).
[29]A. J. Greenfield, Phys. Rev. Letters 16, 6 (1966).
[30]A. Paskin, in Ref. 8.
[31]R. R. Fessler, R. Kaplow, and B. L. Averbach, Phys. Rev. 150, 34 (1966).

Microscopic Quantum Hydrodynamics for Interacting Bose Systems

Robert Fanelli and R. E. Struzynski
Brooklyn College of the City University of New York, Brooklyn, New York
(Received 1 April 1968)

Two equivalent microscopic formulations of quantum hydrodynamics are developed. Commutation rules for hydrodynamical quantities are developed, and in particular, the commutation rule for components of the fluid velocity operator is found to be in disagreement with that derived by Landau. Vortex quantization is found to be a natural consequence of the theory.

I. INTRODUCTION

Theoretical investigations of superfluidity in Bose systems have been characterized by two major approaches, which we call the statistical approach and the quantum-hydrodynamical approach. The former[1] assumes the existence, in the superfluid state, of a statistical order parameter which is usually associated with an expectation value of the field, ψ. The order parameter is complex and the superfluid velocity, $\vec{v}_S$, is associated with the gradient of its phase. The quantization of circulation first suggested by Onsager[2] thus follows from the theory. Quantum hydrodynamics, on the other hand, involves defining a specific operator for the superfluid velocity. It was originated by Landau[3] and further developed by Pitaevskii.[4] An alternative version of it was developed by Kronig, Thellung, and Ziman.[5] The aim of this paper is to reexamine the quantum hydrodynamics of Landau, clothe it in more modern dress, and try to draw some new conclusions from it.

The main results of our analysis are the following:

(a) Quantum hydrodynamics is presented in a second-quantized formulation and the commutator of the components of the velocity operator is found to be zero, in contradiction to the result of Landau.

(b) A field-theoretic formulation based on density and phase operators is shown to be equivalent to quantum hydrodynamics with the velocity operator as the gradient of the phase operator.

(c) The velocity operator is shown to obey the quantization-of-circulation condition.

By way of introduction, we here give a brief review of quantum hydrodynamics. Describing the Bose fluid in terms of many-particle wave functions, Landau introduced a density operator and a mass current density operator

$$\rho(\vec{r}) = \sum_{i=1}^{N} m_i \delta(\vec{r}-\vec{r}_i) \tag{1.1}$$

and

$$\vec{j}(\vec{r}) = \frac{\hbar}{2i} \sum_{i=1}^{N} [\nabla_i \delta(\vec{r}-\vec{r}_i) + \delta(\vec{r}-\vec{r}_i)\nabla_i], \tag{1.2}$$

respectively. He defined a Hermitian velocity operator as

$$\vec{v}(\vec{r}) = \tfrac{1}{2}[\rho^{-1}(\vec{r})\vec{j}(\vec{r}) + \vec{j}(\vec{r})\rho^{-1}(\vec{r})]. \tag{1.3}$$

The most notable among the commutation relations between these operators is

$$[v_x(\vec{r}), v_y(\vec{r}')] = -i\hbar\delta(\vec{r}-\vec{r}')\rho^{-1}(\vec{r})[\nabla\times\vec{v}(\vec{r})]_z. \tag{1.4}$$

He further introduced a quasimacroscopic hydrodynamic Hamiltonian given by

$$H = \int d\vec{r}\{\tfrac{1}{2}\vec{v}(\vec{r})\cdot\rho(\vec{r})\vec{v}(\vec{r}) + E[\rho(\vec{r})]\}, \tag{1.5}$$

where $E[\rho]$ is an unspecified functional of ρ. From this Hamiltonian he obtained hydrodynamic Heisenberg equations for ρ and $\vec{v}$, i.e.,

$$\dot{\rho} = -\nabla\cdot\vec{j} \tag{1.6}$$

$$\dot{\vec{v}} = -[v_k(\partial v_i/\partial x_k) + (\partial v_i/\partial x_k)v_k] - \rho^{-1}\nabla[\rho^2(\partial/\partial\rho)(E\rho^{-1})]. \tag{1.7}$$

Later, Pitaevskii[4] deduced directly from quantum hydrodynamics the existence of an excitation spectrum.

Kronig, Thellung, and Ziman[5] constructed an alternative quantum hydrodynamics by quantizing a Hamiltonian formulation of the dynamics of a classical fluid, treated as a continuum. They obtained similar commutators and equations of motion to those of Landau. In order to obtain Eq. (1.4), they had to define the fluid velocity as the gradient of a velocity potential plus extra terms, thus arbitrari-